IEEE Access
Multidisciplinary | Rapid Review | Open Access Journal

Received September 11, 2021, accepted September 23, 2021, date of publication September 27, 2021,
date of current version October 8, 2021.

Digital Object Identifier 10.1109/ACCESS.2021.3115948

H_∞ Output-Feedback Anti-Swing Control for a Nonlinear Overhead Crane System With Disturbances Based on T-S Fuzzy Model

CHENGCHENG LI, YUXIANG XIA, AND WENXUAN WANG
School of Mechatronics Engineering, Lanzhou Jiaotong University, Lanzhou 730070, China

Corresponding author: Yuxiang Xia (yuxiangxia0305@126.com)

This work was supported in part by the Natural Science Foundation of Gansu Province under Grant 20JR10RA265 and Grant 20JR10RA269, in part by the Youth Natural Science Foundation of Lanzhou Jiaotong University under Grant 2020043, in part by the Tianyou Youth Talent Lift Program of Lanzhou Jiaotong University, and in part by the Higher Education Innovation Foundation of Gansu Province under Grant 2021B-112.

ABSTRACT In this paper, the H_∞ output-feedback controller for a nonlinear overhead crane system with external disturbances was developed. Firstly, the Takagi-Sugeno fuzzy model was used to represent the overhead crane system nonlinearity. A fuzzy-based state observer was then built to estimate the values of immeasurable variables. Secondly, a novel control design called virtual-desired variable synthesis was used to converting the tracking control into a stabilization problem. It was primarily used to define the internal desired states, making the design procedure clear and easy. The H_∞ performance criterion was used to attenuate external disturbances, and the closed-loop model stability was investigated using the quadratic Lyapunov function. Finally, three simulations were conducted to verify the feasibility and effectiveness of the proposed method. The results have shown that there is practically no positioning error and residual payload swing. Thus, in theory, any type of bounded external disturbances can be eliminated using the proposed method. Additionally, the convergence time is half of its model predictive control method counterpart and one-third of the standard H_∞ controller. Hence, it provides a reference for actual control of the overhead crane systems, mostly due to its good performance.

INDEX TERMS Overhead crane, output feedback, T-S fuzzy model, virtual-desired variable synthesis.

I. INTRODUCTION

The crane systems are widely used due to their advantages, including the low energy consumption, simple mechanical structure, and high load capacity. Thus, both the safety and work efficiency of overhead crane systems must be guaranteed. The anti-swing and fast positioning properties in particular are considered to be the most important industrial crane characteristic. However, fast trolley positioning and small payload swing are conflicting requirements mostly due to the high coupling between the payload swing and the trolley acceleration or deceleration. Such systems include but are not limited to: inverted pendulum, gymnast robot, and offshore crane, among others, are underactuated mechanical systems [1]–[5]. They have fewer control inputs than degrees of freedom, which makes their control significantly more challenging.

During the crane system transportation, payload oscillations may cause safety hazards, reduce the working efficiency, or make unloading more difficult. Furthermore, since cranes are generally used in the outdoor environment, external disturbances are hard to avoid. For this reason, the development of suitable control techniques aiming to reduce the payload sway and improve the system efficiency in the presence of external disturbances is a topic of great interest for both academia and industry.

One of the more widely utilized methods is the input shaping technique [6], which is an effective open-loop control method for swing reduction and crane system positioning. Many other open-loop strategies were also proposed for crane control [7], [8]. However, the base assumption in open-loop methods is that the system information must be known, meaning that their control performance can be easily

The associate editor coordinating the review of this manuscript and approving it for publication was Choon Ki Ahn.

influenced by nonlinearity, initial conditions, and external disturbances. The feedback control method was proven to be more robust regarding the modeling errors, parameter uncertainties, and extraneous disturbances compared to open-loop control. Recently, various control approaches were proposed based on feedback control. A study was carried out aiming to find the optimal motion planning solution in terms of overhead crane energy efficiency [9]. Moreover, a swing constraint guaranteed model predictive control (MPC) algorithm was proposed for use in under-actuated overhead cranes [10]. Next, a continuous robust control method was designed for the crane system trajectory tracking control was presented in [11]. However, in these methods the mathematical model of the overhead crane system was linearized to an approximate model, meaning that the system non-linearity was neglected during the control process.

An enhanced coupling control scheme based on the crane system passivity property was proposed in [12], guaranteeing similar payload swing amplitudes for various transportation tasks. In [13], an emergency braking method was devised to avoid undesired accidents of the overhead crane system. Furthermore, a finite-time trajectory tracking control method was proposed for overhead crane systems in [14]. In [15], the authors proposed a fault-tolerant control strategy based on the T-S fuzzy model, which was applied in overhead cranes. Additionally, many other techniques were used in the crane control, such as partial feedback linearization [16], MPC [17], and independent joint control strategy [18], among others. However, external disturbances are neglected in all the listed methods.

After carefully reviewing the existing crane control studies, the authors found that the crane system control problem remains a fairly open topic. There are two issues that need to be solved: (1) For the control design convenience, several existing approaches were based on the linearized dynamic model or making approximation operations to the crane dynamic model when performing stability analysis. (2) The existing fuzzy control methods for the crane control were utilized to deal with the model non-linearity, however, external disturbances were not considered.

Aiming to address the above-presented issues, inspired by the existing literature [10] and [15], in this paper the authors studied the anti-swing control based on H_∞ output-feedback design. The T-S fuzzy approach was used to approximate the crane non-linearity. The internal part states, including premise variables, were assumed to be immeasurable and were estimated by a fuzzy observer. Further, the new concepts, virtual desired variables, and in turn generalized kinematic constraint were used to make the design procedure clear and easy. Based on the newly developed controller, external disturbances were eliminated by applying H_∞ criterion.

To sum up, the scientific contribution of the paper is as follows:

1) A novel concept of virtual desired variables was used in this paper to make the design procedure clear and easy, which transferred the tracking problem into the stability issues and relaxed the need for a real reference model.
2) Combining with T-S fuzzy model, the H_∞ criterion were applied to eliminate external disturbances, which improved the transient control performance and enhanced the system robustness.
3) Not only the proposed method obtained better performance under different disturbances, but also it had a simpler structure and fewer variables to be measured due to the application of the parallel distributed compensation (PDC) law with a fuzzy observer, which better fitted the demands of actual control of the crane and provided a feasible idea for the crane control.

The paper at hand is structured as follows: the nonlinear model for the overhead crane was shown in Section 2. The controller design using a T-S fuzzy model, along with the closed-loop system stability conditions were given in Section 3. Finally, the simulation verification was shown in Section 4, while the conclusions were given in Section 5.

Notations: In this paper, R^n and $R^{n\times m}$ represent the n-dimensional Euclidean space and the set of all $n \times m$ real matrices, respectively. Further, $(P > 0(\geq 0))$ denotes that matrix P is real symmetric and positive definite (semidefinite). Superscripts '-1'and 'T' represent the matrix inverse and transpose, respectively. I is the identity matrix with appropriate dimensions, $(*)$ is the symmetric part in the symmetric matrix. The symbols $\|\cdot\|$ denotes the Euclidean norm (for vectors) and induced 2-norm (for matrices). Finally, if their dimensions are not explicitly defined, matrices are assumed to have appropriate dimensions.

II. OVERHEAD CRANE MATHEMATIC MODEL

The main component of overhead crane plant is the trolley, on which the payload is suspended by a rope. The typical overhead crane is shown in Figure 1. The significant parameters used in this section are:

1) M: the total trolley mass (unit: kg),
2) m: the payload mass (unit:kg),
3) l: the rope length (unit:m),
4) g: the gravitational acceleration (unit:m/s^2),

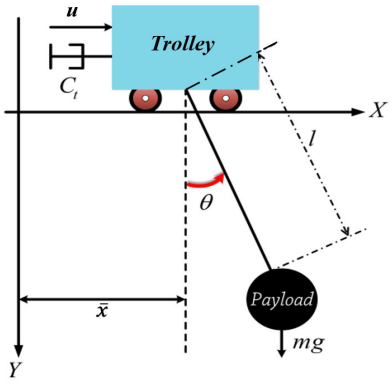

FIGURE 1. The two-dimensional overhead crane system schematics.

5) θ: the load swing angle with respect to the vertical line (unit: rad),
6) $\bar{x}$: the trolley position with respect to the original point (unit:m),
7) u: the driving force acting upon the trolley (unit: N),
8) C_t: the viscous friction coefficient of trolley (unit: Ns/m),
9) d: the external disturbance term (unit: N).

The dynamical 2-D model of the overhead crane plant can be formulated as follow:

$$(M+m)\ddot{\bar{x}} + ml\left(\ddot{\theta}\cos\theta - \dot{\theta}\sin\theta\right) = u - C_t\dot{\bar{x}} + d \quad (1a)$$

$$m\ddot{\bar{x}}\cos\theta + ml\ddot{\theta} + mg\sin\theta = 0 \quad (1b)$$

Aiming to find the state space expression of (1), the state vector $x = [x_1 x_2 x_3 x_4]^T = [\bar{x}\theta\dot{\bar{x}}\dot{\theta}]^T$ is chosen, where u is the control variable. The state-space representation of the overhead crane is written as follows. For the detailed derivation process of the expression, please see Appendix A.

$$\begin{bmatrix}\dot{x}_1\\ \dot{x}_2\\ \dot{x}_3\\ \dot{x}_4\end{bmatrix} = \begin{bmatrix} 0 & 0 & 1 & 0\\ 0 & 0 & 0 & 1\\ 0 & \dfrac{mg\cos x_2\sin x_2}{(M+m\sin^2 x_2)x_2} & \dfrac{-C_t}{M+m\sin^2 x_2} & \dfrac{mlx_4\sin x_2}{M+m\sin^2 x_2}\\ 0 & \dfrac{-(M+m)g\sin x_2}{l(M+m\sin^2 x_2)x_2} & \dfrac{C_t\cos x_2}{l(M+m\sin^2 x_2)} & \dfrac{-mx_4\sin x_2\cos x_2}{M+m\sin^2 x_2}\end{bmatrix} + \begin{bmatrix}0\\0\\ \dfrac{1}{M+m\sin^2 x_2}\\ \dfrac{-\cos x_2}{l(M+m\sin^2 x_2)}\end{bmatrix} u + \begin{bmatrix}0\\0\\ \dfrac{d}{M+m\sin^2 x_2}\\ \dfrac{-d\cos x_2}{l(M+m\sin^2 x_2)}\end{bmatrix} \quad (2)$$

Assuming that angle θ is small and the expression $\lim_{x_2\to 0}\frac{\sin x_2}{x_2} = 1$, the state equation (2) can be written as follows:

$$\begin{bmatrix}\dot{x}_1\\ \dot{x}_2\\ \dot{x}_3\\ \dot{x}_4\end{bmatrix} = \begin{bmatrix} 0 & 0 & 1 & 0\\ 0 & 0 & 0 & 1\\ 0 & \dfrac{mg\cos x_2}{M+m\sin^2 x_2} & \dfrac{-C_t}{M+m\sin^2 x_2} & \dfrac{mlx_4\sin x_2}{M+m\sin^2 x_2}\\ 0 & \dfrac{-(M+m)g}{l(M+m\sin^2 x_2)} & \dfrac{C_t\cos x_2}{l(M+m\sin^2 x_2)} & \dfrac{-mx_4\sin x_2\cos x_2}{M+m\sin^2 x_2}\end{bmatrix} + \begin{bmatrix}0\\0\\ \dfrac{1}{M+m\sin^2 x_2}\\ \dfrac{-\cos x_2}{l(M+m\sin^2 x_2)}\end{bmatrix} u + \begin{bmatrix}0\\0\\ \dfrac{d}{M+m\sin^2 x_2}\\ \dfrac{-d\cos x_2}{l(M+m\sin^2 x_2)}\end{bmatrix} \quad (3)$$

Equation (2) can also be rewritten as:

$$\dot{x}(t) = Ax(t) + Bu(t) + D(t) \quad (4a)$$

$$y(t) = Cx(t) + \upsilon(t) \quad (4b)$$

where:

$$A = \begin{bmatrix} 0 & 0 & 1 & 0\\ 0 & 0 & 0 & 1\\ 0 & \dfrac{mg\cos x_2}{M+m\sin^2 x_2} & \dfrac{-C_t}{M+m\sin^2 x_2} & \dfrac{mlx_4\sin x_2}{M+m\sin^2 x_2}\\ 0 & \dfrac{-(M+m)g}{l(M+m\sin^2 x_2)} & \dfrac{C_t\cos x_2}{l(M+m\sin^2 x_2)} & \dfrac{-mx_4\sin x_2\cos x_2}{M+m\sin^2 x_2}\end{bmatrix},$$

$$B = \begin{bmatrix}0\\0\\ \dfrac{1}{M+m\sin^2 x_2}\\ \dfrac{-\cos x_2}{l(M+m\sin^2 x_2)}\end{bmatrix}, D(t) = \begin{bmatrix}0\\0\\ \dfrac{d}{M+m\sin^2 x_2}\\ \dfrac{-d\cos x_2}{l(M+m\sin^2 x_2)}\end{bmatrix},$$

$$C = \begin{bmatrix}1&0&0&0\\0&1&0&0\\0&0&0&0\\0&0&0&0\end{bmatrix}$$

It should be noted that $\upsilon(t)$ represents the measurement noise.

Assumption 1: $D(t)$ is the unknown bounded disturbance and $\|D(t)\| \le \vartheta$, ϑ is a positive constant.

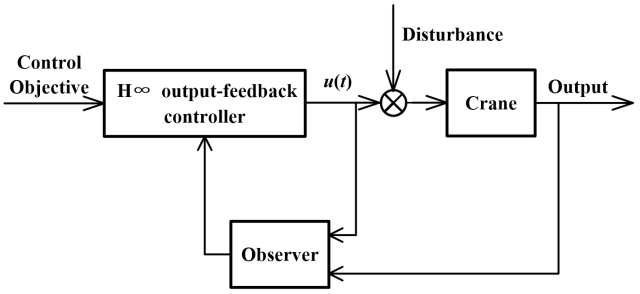

FIGURE 2. Overall H∞ output-feedback controller block diagram.

Please note that (4) is a general non-linear model with a four state variables and one control input. In the following paragraphs, our purpose is to design an H_∞ output feedback control method so that the state variables tracked the desired trajectory. The controller block diagram is given in Figure 2. In the next step, the simulation was carried out on the existing overhead crane plant.

This paper aims to design a control input u so that the output x_1 converges to a specified constant as accurately as possible, which represents the trolley position. Furthermore, the output x_2 converges to zero, which represents the swing angle of the load, despite the disturbance and non-linearity.

III. H∞ OUTPUT-FEEDBACK CONTROLLER DESIGN

A. T-S FUZZY MODELS

T-S fuzzy models are utilized to approximate the non-linear system by expressing it as a set of linear time-invariant (LTI) models. The LTI models are connected by a set of non-linear functions. Each rule associates an LTI model

(as a concluding part) to a weight function obtained using premises given in [19]. In this paper, the authors focused on the T-S fuzzy models with external disturbances which was unknown but bounded. The disturbances were included in each of LTI models [20].

Therefore, the i-th rule can be expressed as:

$$\text{Rule } i: \text{ if } z_1(t) \text{ is } F_{1i} \text{ and } z_2(t) \text{ is } F_{2i} \text{ and } z_3(t) \text{ is } F_{3i} \text{ then } \begin{cases} \dot{x}(t) = A_i x(t) + B_i u(t) + D(t) \\ y(t) = Cx(t) + \upsilon(t) \end{cases} \tag{5}$$

where $z(t) = [z_1(t), z_2(t), z_3(t)]$, are the premise variables consisting of the system states; $F_{ji}(j = 1, 2, 3)$ are the fuzzy sets; $i = 2^3$ is the number of the fuzzy rules, and A_i, B_i are system matrices with appropriate dimensions. $\mu_i(z(t)) = w_i(z(t))/\sum_i^r w_i(z(t))$ with $w_i(z(t)) = \prod_{j=1}^3 F_{ji}$, Note that $\sum_{i=1}^r \mu_i(z(t)) = 1$ for all t, where $\mu_i(z(t)) \geq 0$, for $i = 1,2,3$ are the normalized weights. For sake of simplicity, $\mu_i(z(t))$ is denoted as μ_i.

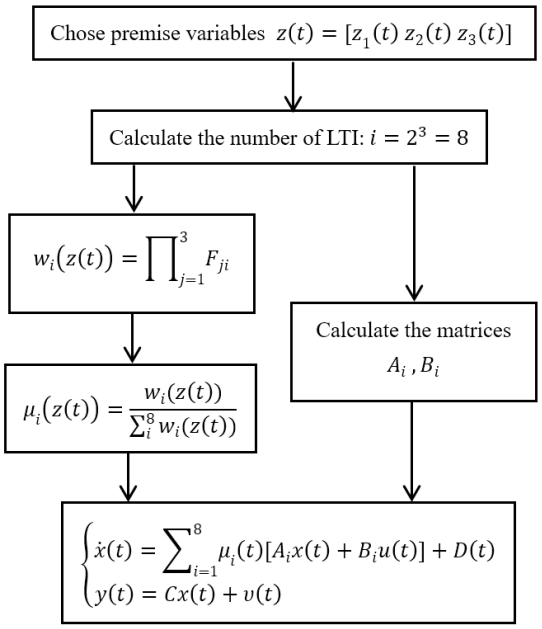

FIGURE 3. Establishment flowchart of the T-S Fuzzy models.

Using a standard fuzzy-inference approach (i.e., a singleton fuzzifier), product fuzzy inference, and weighted average defuzzifier, the calculation yields the following compact presentation of Equation (5):

$$\begin{cases} \dot{x}(t) = A(\mu)x(t) + B(\mu)u(t) + D(t) \\ y(t) = Cx(t) + \upsilon(t) \end{cases} \tag{6}$$

where:

$$\begin{cases} A(\mu) = \sum_{i=1}^8 \mu_i A_i \\ B(\mu) = \sum_{i=1}^8 \mu_i B_i \\ \mu := \mu(t) = [\mu_1, \ldots, \mu_8] \end{cases} \tag{7}$$

The establishment flowchart of the T-S Fuzzy models is shown as Figure 3:

An additional observer is included to estimate the immeasurable variables, such as the velocity x_3 and angular velocity x_4. It is based on the nominal model and has the general form as follows:

$$\begin{cases} \dot{\hat{x}}(t) = A(\mu)\hat{x}(t) + B(\mu)u(t) + L(\mu)(y(t) - \hat{y}(t))] \\ \hat{y}(t) = C\hat{x}(t) \end{cases} \tag{8}$$

where $\hat{x}(t)$ is the estimated state and $L(\mu) = \sum_{i=1}^r \mu_i L_i$ is the observer gain for the i-th LTI model.

B. $H\infty$ OUTPUT-FEEDBACK CONTROLLER

In order to convert the tracking problem into the stability issues, we introduce a set of virtual desired variables x_d which will be tracked by the state variable x [21]. Define $e_d(t) = x(t) - x_d(t)$ to describe the tracking error of the state variables. Then, by combining it with Equation (6), the time derivative of $e_d(t)$ can be obtained:

$$\begin{aligned} \dot{e}_d(t) &= \dot{x} - \dot{x}_d(t) = A(\mu)x(t) + B(\mu)u(t) \\ &\quad -\dot{x}_d(t) + D(t) \end{aligned} \tag{9}$$

It is assumed that the control input $u(t)$ satisfy the follow equation:

$$B(\mu)u_k(t) = B(\mu)u(t) + A(\mu)x_d(t) - \dot{x}_d(t)) \tag{10}$$

where $u_k(t)$ is a new controller to be designed, then the tracking error system (9) can be rewritten as the following form:

$$\begin{cases} \dot{e}_d(t) = A(\mu)e_d(t) + B(\mu)u_k(t) + D(t) \\ y(t) = Cx(t) + \upsilon(t) \end{cases} \tag{11}$$

For the error system (11), we can find that the design of the new control $u_k(t)$ is similar to solve a stabilization problem. Our control purpose is to steer $e_d(t)$ to zero, which means that the state $x(t) - x_d(t)$ converges to zero. The classical structure of a PDC law [22] employed to design the new control law sharing the same nonlinear functions as the T-S model:

$$u_k(t) = K(\mu)(x_d(t) - \hat{x}(t)) \tag{12}$$

where $K(\mu) = \sum_{i=1}^r \mu_i K_i$ represent feedback gains.

Combining the Equation (12) and Equation (11), the following closed-loop error model can be obtained after some simple calculations:

$$\dot{e}_d(t) = (A(\mu) - B(\mu)K(\mu))e_d(t) + B(\mu)K(\mu)e(t) + D(t) \tag{13}$$

Here, the state estimation error was defined as $e(t) = x(t) - \hat{x}(t)$. Taking the derivative of $e(t)$, we obtain:

$$\begin{aligned} \dot{e}(t) &= \dot{x}(t) - \dot{\hat{x}}(t) \\ &= A(\mu)x(t) + B(\mu)u(t) + D(t) \\ &\quad -(A(\mu)\hat{x}(t) + B(\mu)u(t) + L(\mu)(y(t) - \hat{y}(t))]) \\ &= (A(\mu) - L(\mu)C)e(t) - L(\mu)\upsilon(t) + D(t) \end{aligned} \tag{14}$$

Combining (13) and (14), the augmented error of the closed-loop system was obtained as follow:

$$\dot{\tilde{x}} = \sum_{i=1}^{r} \sum_{j=1}^{r} \mu_i(z(t))\,\mu_j(z(t))\,[\tilde{A}_{ij}\tilde{x} + \tilde{S}\tilde{\omega}(t)] \quad (15)$$

with

$$\tilde{x}(t) = \begin{bmatrix} e_d(t) \\ e(t) \end{bmatrix}$$

$$\tilde{A}_{ij} = \begin{bmatrix} A(\mu) - B(\mu)K(\mu) & B(\mu)K(\mu) \\ 0 & A(\mu) - L(\mu)C \end{bmatrix}$$

$$\tilde{S} = \begin{bmatrix} I & 0 \\ I & -L(\mu) \end{bmatrix}, \tilde{\omega}(t) = \begin{bmatrix} D(t) \\ \upsilon(t) \end{bmatrix}$$

Actually, $\tilde{\omega}(t)$ represents the comprehensive disturbances that will deteriorate the control performance and even lead to instability of the closed-loop system. Due to H_∞ criterion is an efficient tool to eliminate the effect of $\tilde{\omega}(t)$ on the control system, so that it will be used to improve the control performance in (15).

The comprehensive disturbances was attenuated by considering the H_∞ criterion related to the tracking error $x(t) - x_d(t)$ as follow [23], [24]:

$$\int_0^{t_f} \left([x(t) - x_d(t)]^T Q [x(t) - x_d(t)] \right) \leq \gamma^2 \int_0^{t_f} (D(t)^T D(t) + \upsilon(t)^T \upsilon(t)) \quad (16)$$

where t_f represents the final time, $Q = Q^T > 0$ denotes a positive definite matrix, and γ is the attenuation level.

By combining (15), the inequality(16) can be written as:

$$\int_0^{t_f} \tilde{x}(t)^T \tilde{Q} \tilde{x}(t) \leq \gamma^2 \int_0^{t_f} \tilde{\omega}(t)^T \tilde{\omega}(t) \quad (17)$$

where $\tilde{Q} = diag[Q0]^T$, $\tilde{\omega}^T\tilde{\omega} = \upsilon(t)^T\upsilon(t) + D(t)^T D(t)$

Theorem 1: For all $t > 0$, $\mu_i(z(t))\,\mu_j(z(t)) \neq 0$. If $\tilde{P} = \tilde{P}^T > 0$, positive constants γ and ε exist, such that the following matrix inequalities hold [25]:

$$\begin{cases} \Upsilon_{ii} < 0 \\ \dfrac{2}{r-1}\Upsilon_{ii} + \Upsilon_{ij} + \Upsilon_{ji} \leq 0, i \neq j \end{cases}$$

with

$$\Upsilon_{ij} = \begin{bmatrix} \tilde{A}^T\tilde{P} + \tilde{P}\tilde{A} + \tilde{Q} & \tilde{P} \\ (*) & -\gamma^2 I \end{bmatrix} \leq 0 \quad (18)$$

Then the closed-loop system asymptotic stability (15) and H_∞ control performance was guaranteed with an attenuation level γ.

Proof: The following candidate Lyapunov function was considered:

$$V(\tilde{x}, t) = \tilde{x}(t)^T \tilde{P} \tilde{x}(t) \;\; with\; \tilde{P} = \tilde{P}^T > 0$$

Using Equation (15), the corresponding time derivative of $V(\tilde{x}, t)$ was obtained as follow:

$$\dot{V}(\tilde{x}, t) = \sum_{i=1}^{r} \sum_{j=1}^{r} \mu_i(z(t))\,\mu_j(z(t))[\tilde{x}^T\tilde{P}\tilde{A}_{ij}\tilde{x} + \tilde{x}^T\tilde{A}_{ij}^T\tilde{P}\tilde{x} + \tilde{x}^T\tilde{P}\tilde{S}\tilde{\omega} + \tilde{\omega}^T\tilde{S}^T\tilde{P}\tilde{x}] \quad (19)$$

By combining (17), if the following inequality holds, the augmented system (15) is asymptotically stable and satisfies the H_∞ requirement with an attenuation level γ:

$$\dot{V}(\tilde{x}, t) + \tilde{x}^T\tilde{Q}\tilde{x} - \gamma^2\tilde{\omega}^T\tilde{\omega} \leq 0 \quad (20)$$

Based on (20), we write:

$$\sum_{i=1}^{r}\sum_{j=1}^{r} \mu_i(z(t))\,\mu_j(z(t))(\tilde{x}^T\tilde{P}\tilde{A}_{ij}\tilde{x} + \tilde{x}^T\tilde{A}_{ij}^T\tilde{P}\tilde{x} + \tilde{x}^T\tilde{P}\tilde{S}\tilde{\omega} + \tilde{\omega}^T\tilde{S}^T\tilde{P}\tilde{x} + \tilde{x}^T\tilde{Q}\tilde{x} - \gamma^2\tilde{\omega}^T\tilde{\omega}) \leq 0$$

and then, the following inequality is obtained:

$$\sum_{i=1}^{r}\sum_{j=1}^{r} \mu_i(z(t))\,\mu_j(z(t))[\tilde{x}(t)^T(\tilde{P}\tilde{A}_{ij} + \tilde{A}_{ij}^T\tilde{P} + \tilde{Q})\tilde{x} + \tilde{x}^T\tilde{P}\tilde{S}\tilde{\omega} + \tilde{\omega}^T\tilde{S}^T\tilde{P}\tilde{x} - \gamma^2\tilde{\omega}^T\tilde{\omega}] \leq 0 \quad (21)$$

and (21) can be rewritten as:

$$\begin{bmatrix} \tilde{x}(t) \\ \tilde{\omega}(t) \end{bmatrix}^T \sum_{i=1}^{r}\sum_{j=1}^{r} \mu_i(z(t))\,\mu_j(z(t)) \begin{bmatrix} \tilde{P}\tilde{A}_{ij} + \tilde{A}_{ij}^T\tilde{P} + \tilde{Q} & \tilde{P}\tilde{S} \\ (*) & -\gamma^2 I \end{bmatrix} \times \begin{bmatrix} \tilde{x}(t) \\ \tilde{\omega}(t) \end{bmatrix} \leq 0 \quad (22)$$

After applying Lemma 2 on inequality (21), Theorem 1 conditions hold.

The object was to obtain a solvable LMI problem so that will the gain matrix K_i can be found. In addition, it is necessary to prove the closed-loop stability (finding $\tilde{P} > 0$) while guaranteeing that the predefined attenuation level γ is achieved.

C. SOLUTION

To find the main results, the following lemmas must be covered.

Lemma 1 [26]: For the given matrices X, Y, $S = S^T > 0$ with compatible dimensions and positive constant β, the following inequalities satisfy:

$$X^TY + Y^TX \leq \alpha X^TX + \alpha^{-1}Y^TY$$

and

$$X^TY + Y^TX \leq X^T\beta X + Y^T\beta^{-1}Y$$

Lemma 2 [27]: For a given symmetric matrix:

$$S = \begin{bmatrix} S_{11} & S_{12} \\ S_{12}^T & S_{22} \end{bmatrix}$$

the following three are equivalent:

(i) $S > 0$;
(ii) $S_{22} < 0, S_{11} - S_{12}S_{22}^{-1}S_{12}^T < 0$;
(iii) $S_{11} < 0, S_{22} - S_{12}^TS_{11}^{-1}S_{12} < 0$;

Lemma 3 [28]: If X <0 be a matrix with compatible dimensions such that $X^T\Omega X \leq 0$ hold, and α is a scalar. In this situation, the following inequality satisfies:

$$X^T\Omega X \leq -\alpha\left(X^T + X\right) - \alpha^2\Omega^{-1}$$

Finally, Theorem 2 gives a solution of the tracking problem for the augmented system (15) with external disturbances.

Theorem 2: For all $t > 0, \mu_i(z(t))\mu_j(z(t)) \neq 0$, if the matrices $P_2 = P_2^T > 0, N = N^T > 0, Y_i, Z_i$, positive constants α, and γ exist, such that the following LMI conditions hold:

$$\begin{cases} \Upsilon_{ii} < 0 \\ \dfrac{2}{r-1}\Upsilon_{ii} + \Upsilon_{ij} + \Upsilon_{ji} \leq 0, i \neq j \end{cases}$$

with

$$\Upsilon_{ij} = \begin{bmatrix} \Lambda(2,2) & -Z_i & P_2 & \alpha I & 0 & 0 & Y_j^T B_i^T & N \\ (*) & -\gamma^2 I & 0 & 0 & \alpha I & 0 & 0 & 0 \\ (*) & (*) & -\gamma^2 I & 0 & 0 & \alpha I & N & 0 \\ (*) & (*) & (*) & -2\alpha N & 0 & 0 & 0 & 0 \\ (*) & (*) & (*) & (*) & -2\alpha N & 0 & 0 & 0 \\ (*) & (*) & (*) & (*) & (*) & -2\alpha N & 0 & 0 \\ (*) & (*) & (*) & (*) & (*) & (*) & \tilde{\Lambda}(1,1) & 0 \\ (*) & (*) & (*) & (*) & (*) & (*) & (*) & -Q^{-1} \end{bmatrix}$$

$$\tilde{\Lambda}(1,1) = \left(A_i - B_i K_j\right) N + N\left(A_i - B_i K_j\right)^T$$

$$\Lambda(2,2) = P_2 A_i - Z_i C_j + A_i^T P_2 - C_j^T Z_i^T \tag{23}$$

Then the augmented system (15) is asymptotically stable and satisfies the H_∞ requirement with an attenuation level γ:

Furthermore, if a solution exists, we can obtain the gain K_i and L_i by using: $K_i = Y_i N^{-1}, L_i = P_2^{-1} Z_i$.

Proof: To simplify the design of controller, $\tilde{P} = diag[P_1, P_2]$ was utilize into the calculation. Inequality (22) was then rewritten as:

$$\sum_{i=1}^{r}\sum_{j=1}^{r} \mu_i \mu_j \tilde{\Theta} \leq 0 \tag{24}$$

with $\tilde{\Theta}$, as shown at the bottom of the page.

Inequality (24) holds if:

$$\sum_{i=1}^{r}\sum_{j=1}^{r} \mu_i \mu_j \begin{bmatrix} \Lambda(1,1) & P_1 B_i K_j & P_1 & 0 \\ (*) & \Lambda(2,2) & P_2 & -P_2 L_i \\ (*) & (*) & -\gamma^2 I & 0 \\ (*) & (*) & (*) & -\gamma^2 I \end{bmatrix} \leq 0 \tag{25}$$

with:

$$\Lambda(1,1) = P_1\left(A_i - B_i K_j\right) + \left(A_i - B_i K_j\right)^T P_1 + Q$$
$$\Lambda(2,2) = P_2\left(A_i - L_i C_j\right) + (A_i - L_i C_j)^T P_2$$

We carry out a simple elementary transformation on matrix (25) to rearrange its order. Firstly, the first and the second row are exchanged, followed by the exchange of the first and the second column. In the next step, the second and the 4th row are switched, followed by the switching of the second and fourth columns. Thus, equation (25) is equivalent to:

$$\sum_{i=1}^{r}\sum_{j=1}^{r} \mu_i \mu_j \begin{bmatrix} \Lambda(2,2) & -P_2 L_i & P_2 & K_j^T B_i^T P_1^T \\ (*) & -\gamma^2 I & 0 & 0 \\ (*) & (*) & -\gamma^2 I & P_1 \\ (*) & (*) & (*) & \Lambda(1,1) \end{bmatrix} \leq 0 \tag{26}$$

In the next step, a bijective change of variables followed by a pre-post multiplication of inequality (26) was carried out by $diag[N, N, N, N]$ with $Y_i = K_i N, N = P_1^{-1}, Z_i = P_2 L_i$. In that case, the inequality (26) was equivalent to:

$$\sum_{i=1}^{r}\sum_{j=1}^{r} \mu_i \mu_j \begin{bmatrix} \begin{bmatrix} N & 0 & 0 \\ 0 & N & 0 \\ 0 & 0 & N \end{bmatrix} & \Xi & \begin{bmatrix} N & 0 & 0 \\ 0 & N & 0 \\ 0 & 0 & N \end{bmatrix} & \begin{matrix} Y_j^T B_i^T \\ 0 \\ N \end{matrix} \\ (*) & (*) & (*) & \tilde{\Lambda}(1,1) \end{bmatrix} \leq 0 \tag{27}$$

with

$$\Xi = \begin{bmatrix} \Lambda(2,2) & -Z_i & P_2 \\ (*) & -\gamma^2 I & 0 \\ (*) & (*) & -\gamma^2 I \end{bmatrix} \tag{28}$$

$$\tilde{\Lambda}(1,1) = \left(A_i - B_i K_j\right) N + N\left(A_i - B_i K_j\right)^T + NQN \tag{29}$$

According to Inequality (27) and Equation (29), it can be known that major requirement for an LMI formulation can be obtained as the product of:

$$\begin{bmatrix} N & 0 & 0 \\ 0 & N & 0 \\ 0 & 0 & N \end{bmatrix} \Xi \begin{bmatrix} N & 0 & 0 \\ 0 & N & 0 \\ 0 & 0 & N \end{bmatrix} \tag{30}$$

Furthermore, by using Lemma 3 to (30), we obtain:

$$\begin{bmatrix} N & 0 & 0 \\ 0 & N & 0 \\ 0 & 0 & N \end{bmatrix} \Xi \begin{bmatrix} N & 0 & 0 \\ 0 & N & 0 \\ 0 & 0 & N \end{bmatrix} \leq -2\alpha \begin{bmatrix} N & 0 & 0 \\ 0 & N & 0 \\ 0 & 0 & N \end{bmatrix} - \alpha^2 \Xi^{-1} \tag{31}$$

By applying Lemma 2 (Schur's complement), (31) can be rewritten as:

$$\begin{bmatrix} \Lambda(2,2) & -Z_i & P_2 & \alpha I & 0 & 0 \\ (*) & -\gamma^2 I & 0 & 0 & \alpha I & 0 \\ (*) & (*) & -\gamma^2 I & 0 & 0 & \alpha I \\ (*) & (*) & (*) & -2\alpha N & 0 & 0 \\ (*) & (*) & (*) & (*) & -2\alpha N & 0 \\ (*) & (*) & (*) & (*) & (*) & -2\alpha N \end{bmatrix} \leq 0 \tag{32}$$

$$\tilde{\Theta} = \begin{bmatrix} P_1\left(A_i - B_i K_j\right) + (A_i - B_i K_j)^T P_1 + Q & P_1 B_i K_j & P_1 & 0 \\ K_j^T B_i^T P_1^T & P_2\left(A_i - L_i C_j\right) + (A_i - L_i C_j)^T P_2 & P_2 & -P_2 L_i \\ P_1 & P_2 & -\gamma^2 I & 0 \\ 0 & L_i^T P_2^T & 0 & -\gamma^2 I \end{bmatrix}$$

After substituting (32) into (27), it is possible to obtain the following inequality:

$$\sum_{i=1}^{r}\sum_{j=1}^{r}\mu_i\mu_j \begin{bmatrix} \Lambda(2,2) & -Z_i & P_2 & \alpha I & 0 & 0 & Y_j^T B_i^T \\ (*) & -\gamma^2 I & 0 & 0 & \alpha I & 0 & 0 \\ (*) & (*) & -\gamma^2 I & 0 & 0 & \alpha I & N \\ (*) & (*) & (*) & -2\alpha N & 0 & 0 & 0 \\ (*) & (*) & (*) & (*) & -2\alpha N & 0 & 0 \\ (*) & (*) & (*) & (*) & (*) & -2\alpha N & 0 \\ (*) & (*) & (*) & (*) & (*) & (*) & \tilde{\Lambda}(1,1) \end{bmatrix} \leq 0 \tag{33}$$

with

$$\tilde{\Lambda}(1,1) = \left(A_i - B_i K_j\right) N + N\left(A_i - B_i K_j\right)^T + NQN$$
$$\Lambda(2,2) = P_2 A_i - Z_i C_j + A_i^T P_2 - C_j^T Z_i^T$$

After applying Lemma 2 (Schur's complement) to diagonal blocks $\tilde{\Lambda}(1,1)$ and $\Lambda(2,2)$, Theorem 2 conditions hold. Such results ensure the augmented system (15) is asymptotically stable, satisfying the H_∞ requirement with an attenuation level γ, therefore completing the proof.

The design steps of the proposed H_∞ output-feedback controller were summarized as follow:

Step 1: Establish the T-S fuzzy models and observer

(1) Establish the T-S fuzzy models according to the number of the premise variable vector $z(t)$.

(2) Establish the fuzzy observer using the T-S fuzzy models.

Step 2: Specify the design parameters

(1) Specify the parameters Q and α to obtain the smallest γ.

(2) Specify the parameters P_2, N, Z_i, Y_i, by solving the LMI (23) and $P_2 > 0, N > 0$ using a classical LMI toolbox.

(3) Specify the crane parameters according to [15]

Step 3: Chose the T-S membership functions.

Step 4: Calculate $\mu_i K_i$ using the parameters obtained from Step 2 (2).

Step 5 Obtain the H_∞ output feedback controller $u(t) = u_k(t) - B^{-1}(\mu)(A(\mu)x_d(t) - \dot{x}_d(t))$ and apply it in Equation (4).

Step 6: Return to Step 5 and continue from the second procedure.

In the following section, a series of simulations will be carried out to evaluate the performance of the proposed control scheme.

IV. SIMULATION VERIFICATION

Finally, the simulation was carried out on the existing overhead crane system (4) aiming to illustrate the effectiveness of the present control method. The MATLAB installed on the Windows 10 operating system (i9-9400f processor core and 16GB of RAM) was used to complete the simulation. The control period T was set to 5 ms.

For simulation, the same crane parameters were used as [15]: $M = 10\text{kg}, m = 4\text{kg}, l = 0.5\text{m}, C_t = 0.1\text{Ns/m}$, and $g = 9.8\text{m/s}^2$. The payload swing angle was assumed to be from the interval $-\pi/12 \leq \theta(t) \leq \pi/12$, and the angle velocity was selected from the range $-\pi/4 \leq \dot{\theta}(t) \leq \pi/4$. Furthermore, $z_1(t) = \frac{1}{M+m\sin x_2}$, $z_2(t) = cosx_2$, $z_3(t) = x_4 \sin x_2$ were premise variables; also, $z_{1,max} = 1/M$, $z_{1,min} = 1/(M + m\sin^2(\pi/12))$, $z_{2,max} = 1$, $z_{2,min} = \cos(\pi/12)$, $z_{3,max} = \frac{\pi}{4}\sin(\pi/12)$, $z_{3,min} = -\frac{\pi}{4}\sin(\pi/12)$. Thus, the non-linear system (4) was represented by the following T-S fuzzy model:

$$\text{Rule } i: \text{ if } z_1(t) \text{ is } F_{1i} \text{ and } z_2(t) \text{ is } F_{2i} \text{ and } z_3(t) \text{ is } F_{3i} \text{ then } \begin{cases} \dot{x}(t) = A_i x(t) + B_i u(t) + D(t) \\ y(t) = Cx(t) + \upsilon(t) \end{cases} \text{ for } i = 1, \ldots, 8.$$

Therefore, the non-linear model (4) was rewritten as:

$$\begin{cases} \dot{x}(t) = \sum_{i=1}^{8} \mu_i(t)\left[A_i x(t) + B_i u(t)\right] + D(t) \\ y(t) = Cx(t) + \upsilon(t) \end{cases} \tag{34}$$

where

$$A_i = \begin{bmatrix} 0 & 0 & 1 & 0 \\ 0 & 0 & 0 & 1 \\ 0 & \dfrac{mgz_2 z_1}{l} & \dfrac{-C_t z_1}{l} & \dfrac{mlz_3 z_1}{l} \\ 0 & \dfrac{-(M+m)gz_1}{l} & \dfrac{C_t z_2 z_1}{l} & \dfrac{-mz_3 z_2 z_1}{l} \end{bmatrix},$$

$$B_i = \begin{bmatrix} 0 \\ 0 \\ z_1 \\ \dfrac{-z_2 z_1}{l} \end{bmatrix}, D(t) = \begin{bmatrix} 0 \\ 0 \\ z_1 d(t) \\ \dfrac{-z_2 z_1 d(t)}{l} \end{bmatrix}$$

To approximate the A_i, B_i, and $D(t)$ non-linarites, the T-S membership functions (35) were obtained following the procedure presented in [29]:

$$F_{1,max} = \frac{z_{1,max} - z_1}{z_{1,max} - z_{1,min}}, F_{1,min} = \frac{z_1 - z_{1,min}}{z_{1,max} - z_{1,min}} \tag{35a}$$

$$F_{2,max} = \frac{z_{2,max} - z_2}{z_{2,max} - z_{2,min}}, F_{2,min} = \frac{z_2 - z_{2,min}}{z_{2,max} - z_{2,min}} \tag{35b}$$

$$F_{3,max} = \frac{z_{3,max} - z_3}{z_{3,max} - z_{3,min}}, F_{3,min} = \frac{z_3 - z_{3,min}}{z_{3,max} - z_{3,min}} \tag{35c}$$

where $z_{1,max}, z_{2,max}, z_{3,max}, z_{1,min}, z_{2,min}$, and $z_{3,min}$, are maximum and minimum $z_1(t), z_2(t), z_3(t)$ values, and $F_{ji}(j = 1, 2, 3, i = 1, \ldots, 8)$ can be found by the functions given above. The F_i value can be calculated through eight (2^3) combinations of F_{1i}, F_{2i} and F_{3i}.

Then, Q and α are chosen to obtain the smallest γ. According to the actual calculation, the closed-loop system dynamics were fixed by selecting

$$Q = 10^{-3} \times \begin{bmatrix} 1 & 0 & 0 & 0 \\ 0 & 1 & 0 & 0 \\ 0 & 0 & 1 & 0 \\ 0 & 0 & 0 & 1 \end{bmatrix}.$$

The parameter α was chosen as: $\alpha = 0.001$. The solutions for P_2, N, Z_i, Y_i, and $\eta = \gamma^2$ can be obtained by

solving the optimization problem (36) using a classical LMI toolbox:

$$\begin{aligned} &min\eta \\ &s.t.\ LMI\ (23)\ and P_2 > 0, N > 0 \end{aligned} \tag{36}$$

Finally, the K_i and L_i were obtained using: $K_i = Y_i N^{-1}$, $L_i = P_2^{-1} Z_i$.

Hence, the Theorem 2 solution was obtained by solving the Matlab LMI toolbox (23). The controller gains $K_1, \ldots, K_8$ and observer gains $L_1, \ldots, L_8$ are as follows:

$$\begin{aligned}
K_1 &= [0.6114, -7.3588, 11.2966, 53.2799], \\
K_2 &= [0.1925, 57.7908, 10.2724, 50.1246], \\
K_3 &= [0.5921, -4.0429, 11.2681, 53.1426], \\
K_4 &= [0.1866, 56.1327, 10.2679, 50.1220], \\
K_5 &= [4.8013, 89.7548, 13.2276, 59.8104], \\
K_6 &= [4.6847, 88.9252, 12.5420, 58.3462], \\
K_7 &= [4.6590, 89.6210, 12.8123, 59.5888], \\
K_8 &= [4.5711, 88.7100, 12.1259, 58.1584],
\end{aligned}$$

$$L_1 = 10^3 \times \begin{bmatrix} 0.3499 & -0.0138 & -0.1162 & 0.8058 \\ 0.0360 & 0.0009 & 0.0083 & -0.0614 \\ -0.1125 & 0.0141 & 0.1277 & -0.8801 \\ 0.8034 & -0.1015 & -0.9007 & 6.3310 \end{bmatrix},$$

$$L_2 = 10^3 \times \begin{bmatrix} 0.0124 & -0.0001 & -0.0004 & 0.0175 \\ 0.0004 & 0.0003 & 0.0134 & -0.0876 \\ 0.0018 & 0.0004 & 0.0364 & -0.1791 \\ 0.0029 & -0.0031 & -0.1977 & 1.3665 \end{bmatrix},$$

$$L_3 = 10^3 \times \begin{bmatrix} 0.1347 & -0.0047 & -0.0391 & 0.2766 \\ 0.0108 & 0.0009 & 0.0088 & -0.0598 \\ -0.0375 & 0.0083 & 0.0803 & -0.5342 \\ 0.2738 & -0.0584 & -0.5461 & 3.7487 \end{bmatrix},$$

$$L_4 = 10^3 \times \begin{bmatrix} 0.0117 & -0.0001 & -0.0002 & 0.0153 \\ 0.0003 & 0.0002 & 0.0124 & -0.0792 \\ 0.0018 & 0.0004 & 0.0354 & -0.1697 \\ 0.0028 & -0.0028 & -0.1857 & 1.2504 \end{bmatrix},$$

$$L_5 = \begin{bmatrix} 109.4636 & 8.3492 & 96.4093 & -129.9774 \\ 139.1790 & 17.6907 & 142.3755 & -252.0236 \\ 109.6152 & 12.0443 & 109.9386 & -183.6378 \\ -97.6762 & -24.0384 & -136.6776 & 371.7241 \end{bmatrix}$$

$$L_6 = \begin{bmatrix} 93.2208 & 6.3503 & 81.9925 & -83.3706 \\ 108.7553 & 15.0148 & 116.6131 & -186.2015 \\ 93.3202 & 10.2465 & 96.0683 & -136.9906 \\ -58.2519 & -20.9469 & -102.2200 & 305.0796 \end{bmatrix}$$

$$L_7 = \begin{bmatrix} 105.3770 & 7.9641 & 93.5615 & -124.1583 \\ 133.3056 & 16.9890 & 138.1884 & -241.3728 \\ 106.1543 & 11.7292 & 108.0437 & -178.8302 \\ -92.8286 & -23.2643 & -133.4601 & 359.8527 \end{bmatrix}$$

$$L_8 = \begin{bmatrix} 62.5890 & 2.9403 & 52.3876 & -42.2253 \\ 65.4404 & 9.0816 & 71.8423 & -113.4604 \\ 59.8406 & 5.9791 & 62.4447 & -85.1251 \\ -27.4757 & -14.9652 & -66.0875 & 230.2727 \end{bmatrix}$$

To complete the process, the viscous friction was considered in the MPC controller and the standard H_∞ controller to ensure that the simulations have equal parameters. The two methods were given as follow:

A. THE STANDARD H_∞ CONTROLLER

To design the standard H_∞ controller, Equation (A.1) from Appendix A had to be linearized around the equilibrium point as:

$$\ddot{x} = \frac{mg}{M}\theta - \frac{C_t}{M}\dot{\bar{x}} + \frac{1}{M}u + \frac{1}{M}d \tag{37a}$$

$$\ddot{\theta} = -\frac{(M+m)\,g}{lM}\theta + \frac{C_t}{lM}\dot{\bar{x}} - \frac{1}{lM}u - \frac{1}{lM}d \tag{37b}$$

It should be noted that the linearized model (37) was accurate enough, and was widely used in crane control design [9], [10]. An integral term was used to eliminate the steady-state error, which was expressed as: $\int (x_d - x)\, dt$. The authors have selected the state vector $x = [x_1 x_2 x_3 x_4 x_5 x_6]^T = [\bar{x}\theta\dot{\bar{x}}\dot{\theta} \int (x_{d1} - x_1)dt \int (x_{d2} - x_2)dt]$, where x_{d1}, x_{d2} are the desired value of x_1, x_2. Thus, the system was rewritten as:

$$\begin{cases} \dot{x} = (A_h + \Delta A_h)\, x + B_1 d + B_2 u \\ z = C_1 x \\ y = x \end{cases} \tag{38}$$

where

$$A_h = \begin{bmatrix} 0 & 0 & 1 & 0 & 0 & 0 \\ 0 & 0 & 0 & 1 & 0 & 0 \\ 0 & \frac{mg}{M} & -\frac{C_t}{M} & 0 & 0 & 0 \\ 0 & -\frac{(M+m)\,g}{lM} & \frac{C_t}{lM} & 0 & 0 & 0 \\ -1 & 0 & 0 & 0 & 0 & 0 \\ 0 & -1 & 0 & 0 & 0 & 0 \end{bmatrix}$$

$$B_1 = B_2 = \begin{bmatrix} 0 & 0 & \frac{1}{M} & \frac{-1}{lM} & 0 & 0 \end{bmatrix}^T$$

$\Delta A_h = E \sum(t) F$ is the uncertain term, $\sum(t)$ is an unknown matrix satisfying $\sum^T \sum \leq I$. In this paper, the following values were selected: $E = B_1, F = C_1, C_1 \in R^{6\times 6}$ is a weighted coefficient matrix, which was chosen as an identity matrix.

The standard H_∞ controller was chosen as:

$$u = K_h x \tag{39}$$

where K_h is gain matrix with the appropriate dimensions.

K_h was obtained by solving Riccati inequalities:

$$\begin{cases} A^T X + XA - X\left(\frac{1}{\varepsilon^2} B_2 B_2^T - B_1 B_1^T\right) X + C_1^T C_1 < 0 \\ X > 0 \\ K_h = -\frac{1}{2\varepsilon^2} B_2^T X \end{cases}$$

where ε is a positive constant (value $\varepsilon = 0.1$ was used in this paper). Finally, the gain matrix K_h is obtained:

$$K_h = [-15.9761, 52.3214, -11.1328, -9.8746, 5.6637, 20.5438]$$

B. THE MPC CONTROLLER

The viscous friction was considered in [10], it was found that the mathematical model has the same form with (37). The system can be rewritten as:

$$\begin{aligned} \dot{x}_m &= A_m x_m + B_{m1} d + B_{m2} u \\ y &= C_m x_m \end{aligned} \tag{40}$$

where

$$A_m = \begin{bmatrix} 0 & 0 & 1 & 0 \\ 0 & 0 & 0 & 1 \\ 0 & \frac{mg}{M} & -\frac{C_t}{M} & 0 \\ 0 & -\frac{(M+m)\,g}{lM} & \frac{C_t}{lM} & 0 \end{bmatrix}$$

$$B_{m1} = B_{m2} = \begin{bmatrix} 0 & 0 & \frac{1}{M} & \frac{-1}{lM} \end{bmatrix}^T$$

In [10], a swing constraints guaranteed generalized predictive control (GPC) method (a type of MPC) is proposed, which converts the swing limit requirement into a restriction for the control input, and uses following optimization approach to deal with the input restrictions:

$$\begin{aligned} &\min_{\Delta U} J = \frac{1}{2}\Delta U^T \Psi \Delta U + \Delta U^T \Omega \\ &s.t.\, M\Delta U \le \gamma \ and \ |F| \le Ma_{max} - mg\theta_{max} \end{aligned} \tag{41}$$

where

$$M = \begin{bmatrix} 1 & 0 & \cdots & 0 \\ -1 & 0 & \cdots & 0 \end{bmatrix}_{2\times N_c}, \gamma = \begin{bmatrix} u_{max} - u(k_i - 1) \\ u_{max} + u(k_i - 1) \end{bmatrix}$$

$$\Psi = 2\phi^T \phi, \Omega = -2\phi^T (R_s - F x_e(k_i))$$

$$a_{max} = \frac{\sqrt{lg}}{T}(\theta_{max} - \sqrt{\theta^2(0) + \frac{l}{g}\dot{\theta}^2(0)})$$

$$R_s(k_i) = \begin{bmatrix} r^T(k_i) & \cdots & r^T(k_i) \end{bmatrix}^T \in R^{4N_p \times 1}$$

$$r = cy(k-1) + (1-c)\, y_f, c = c_0 \exp(-\lambda (kT)^2)$$

Other parameters such as $F \in R^{4N_p \times 4}$, $\phi \in R^{4N_p \times N_c}$ were not list here due to space limitation, which can be obtained from A_m, B_m, and C_m.

The swing angle constraint was written as $|\theta(t)| \le \theta_{max}$, where $\theta_{max} = 6°$. Moreover, the constant is $c_0 = 0.7$, $\lambda = 1$, $T = 5ms$, and the initial crane system state is selected as $x_{m,0} = [0000]^T$. The target trolley position is $x_{d1} = 0.4m$. N_p and N_c ($N_c \le N_p$), representing the prediction and the control horizon, respectively, are chosen as : $N_c = 2$, $N_p = 5$ by multiple trials.

The Hildreth's quadratic programming procedure in [30] was utilized to solve the constrained optimization problem (41), so that the optimal ΔU at sampling time k_i can be obtained. Therefore, according to follow equation, the actual change of the system control input can be obtained.

$$\Delta u(k_i) = K^T \Delta U, K = [1, 0, \ldots, 0]^T \in R^{N_c \times 1}$$

Repeat these steps and trolley can be driven to destination with practically no positioning error and no residual payload, while the input amplitude constraints at each sampling time are also ensured.

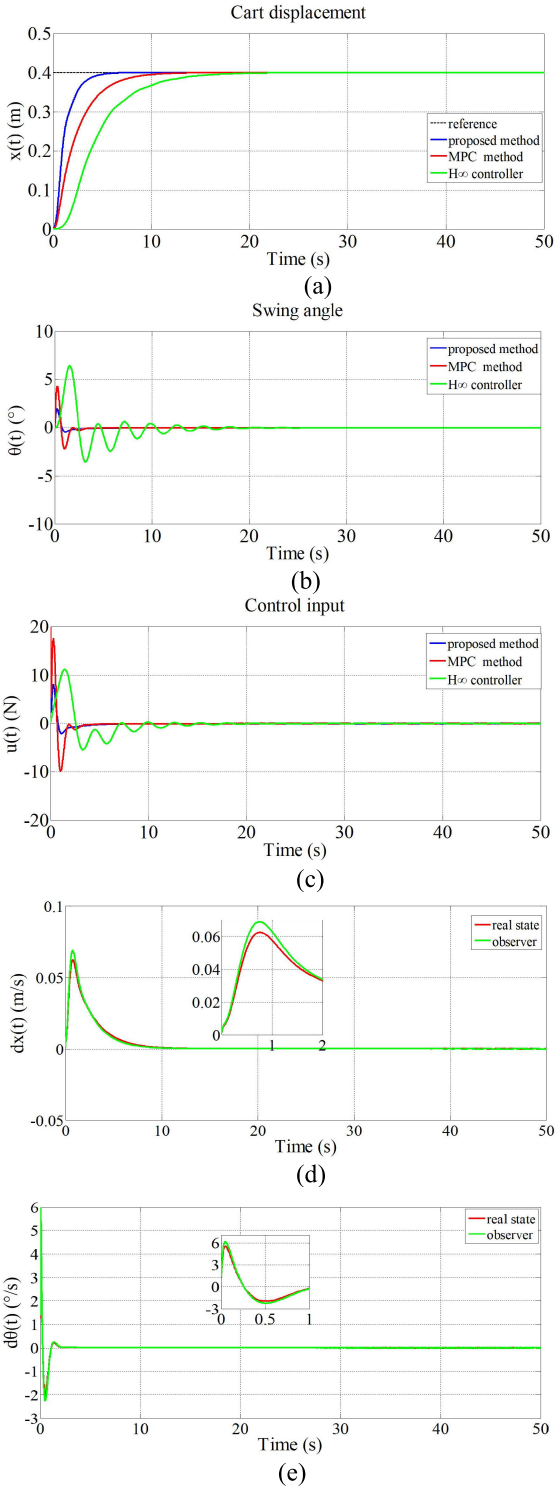

FIGURE 4. Comparison of the proposed method, existing MPC method, and standard H∞ controller for case 1. Black dashed lines represent the reference, blue solid lines show the results obtained by the proposed method, red solid lines show the results by the MPC method. Finally, green solid lines show the results obtained using the standard H∞ controller. (a) position. (b) swing angle. (c) control input using the three methods. (d) observed state of velocity. (e) observed state of swing angular velocity.

Aiming to evaluate the proposed method, it was compared to the MPC controller and the standard H_∞ controller. The comparison was used to illustrate the effectiveness of the proposed control method in the disturbance elimination. Now, simulation and comparison were provided in three different cases: 1) the simulation was conducted without any disturbances to illustrate the positioning performance and the anti-swing ability; 2) a synthesised external disturbance was chosen to evaluate the performance under general disturbance condition; 3) two disturbance inputs were imposed on the crane to assess the performance under the transient pulse disturbance; 4) two disturbance inputs were imposed on the playload; 5) a comprehensive disturbance signal was used, in which the synthesised external disturbance in Case 2 was imposed on crane and the two disturbance inputs in Case 4 was imposed on playload simultaneously.

In Case 1, the trolley travels with a load from 0 to 0.4m. The $\upsilon(t)$ was selected as a normal disturbance, with mean zero and variance one, $d(t)$ was chosen as $d(t) = 0$.

The closed-loop overhead crane outputs and the corresponding control efforts for three approaches were illustrated in Figure 4. Based on the obtained results, it is evident that the trolley can be driven to a specific point with practically no positioning error and no residual payload swing under both the existing MPC method and the proposed method; however, the higher swing angle oscillation was found during the first 20s when using standard H_∞ controller.

By comparing three methods (see Figure 4), it was observed that the existing MPC method drives the cart approximately 10 s from the initial point to the desired point. The standard H_∞ controller reached it in roughly 18s. For the same transportation task, only considering the proposed control method, it required 5 s to drive the cart to the desired location. Additionally, the control input amplitude of the proposed method was the smallest of the three observed methods. The oscillation was also the smallest when the proposed method was used. The results of this case show that the transient-response performance of the proposed control method was better compared to the other two methods. Figure 4(d) and (e) illustrate the observed state of velocity and swing angular velocity.

In Case 2, in addition to keeping the original settings, without loss of generality the unknown but bounded disturbances was taken as follow [31], [32]:

$$d(t) = 20\cos(0.25t) + 20\sin(0.125t) + 20\exp(-0.5t) + 10\text{N}.$$

Based on the obtained results (Figure 5), it was observed that there were practically no positioning errors and no residual payload swing when using the proposed control method. Unfortunately, the highest residual payload swing exists during the whole simulation process by using the standard H_∞ controller. The comparison results in this case show that the proposed method has the best disturbance elimination

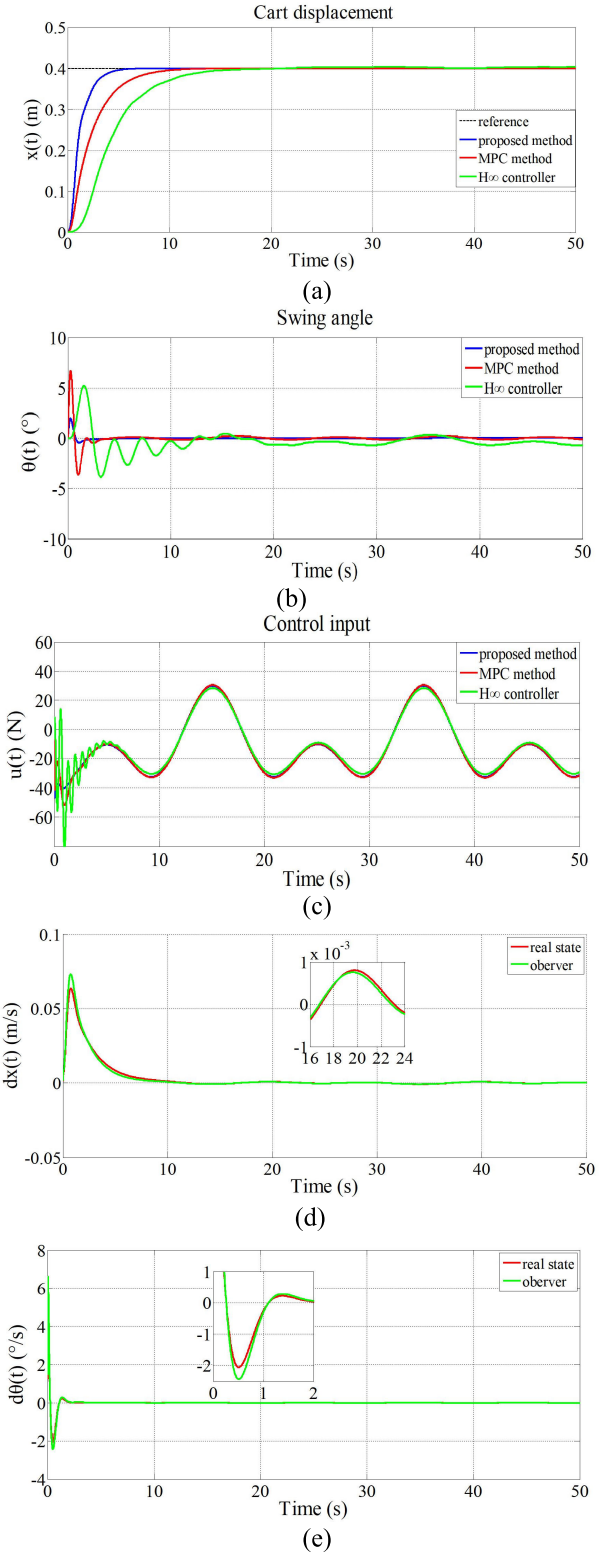

FIGURE 5. Comparison of the proposed method, the existing MPC method, and the standard H∞ controller for case 2. Black dashed lines represent the reference, blue solid lines show the proposed method, and red solid lines results using the MPC method. Finally, green solid lines) are results using the standard H∞ controller. (a) position. (b) swing angle. (c) control input using the three methods. (d) observed state of velocity. (e) observed state of swing angular velocity.

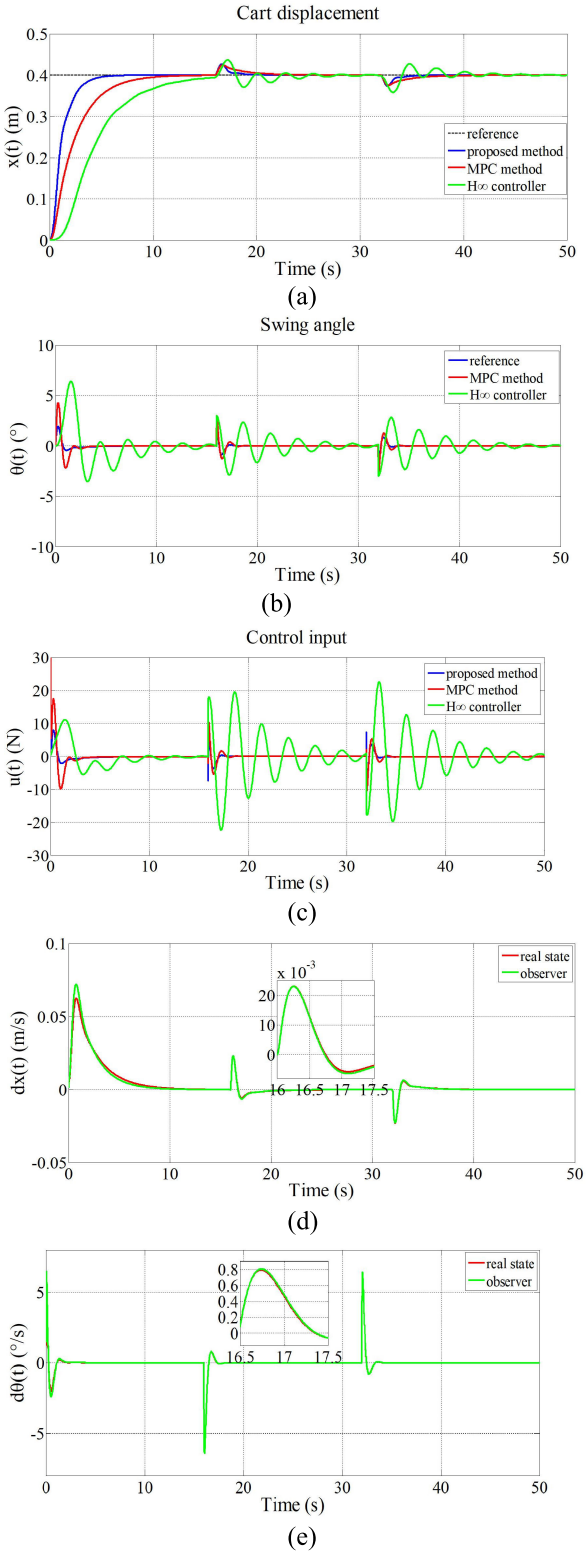

FIGURE 6. Comparison of the proposed method, existing MPC method, and standard H∞ controller for case 3; black dashed lines represent the reference, while the blue solid lines show the proposed method results. Red solid lines show the MPC method results, and the green solid lines results are representing the standard H∞ controller. (a) position. (b) swing angle. (c) control input using the three methods. (d) observed state of velocity. (e) observed state of swing angular velocity.

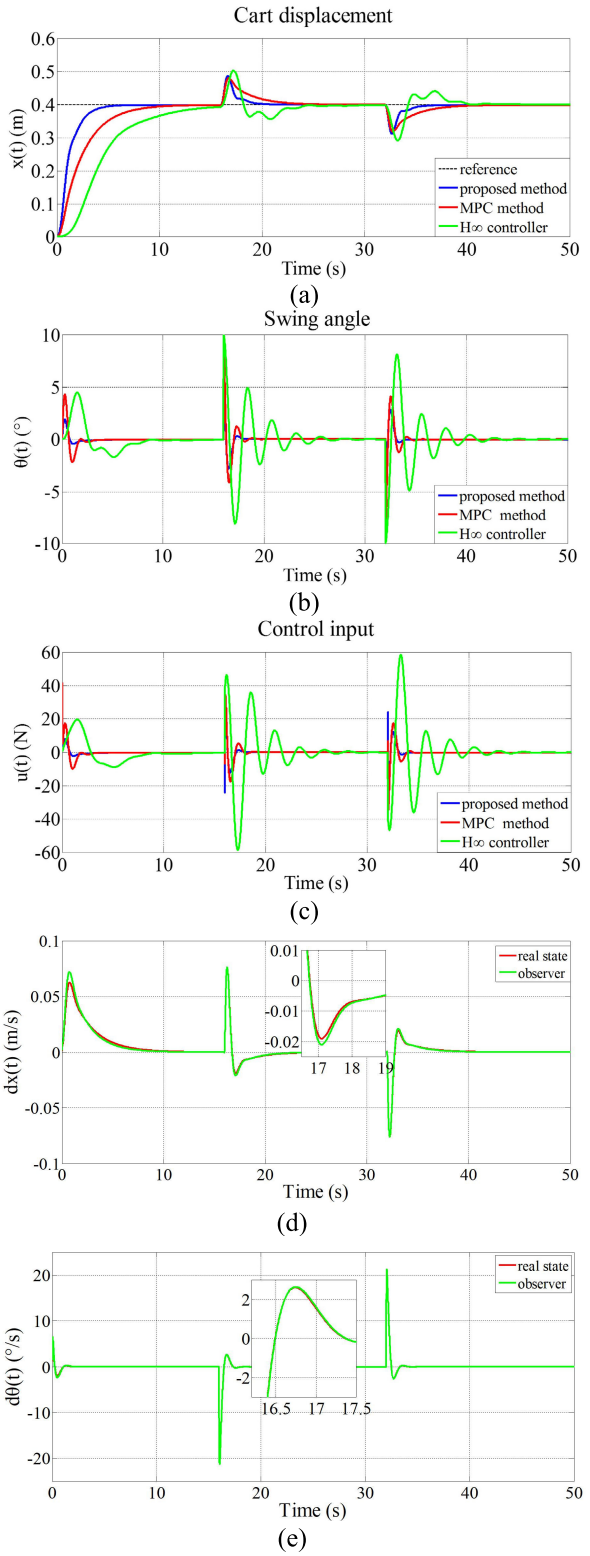

FIGURE 7. Comparison of the proposed method, existing MPC method, and standard H∞ controller for case 4; black dashed lines represent the reference, while the blue solid lines show the proposed method results. Red solid lines show the MPC method results, and the green solid lines results are representing the standard H∞ controller. (a) position. (b) swing angle. (c) control input using the three methods. (d) observed state of velocity. (e) observed state of swing angular velocity.

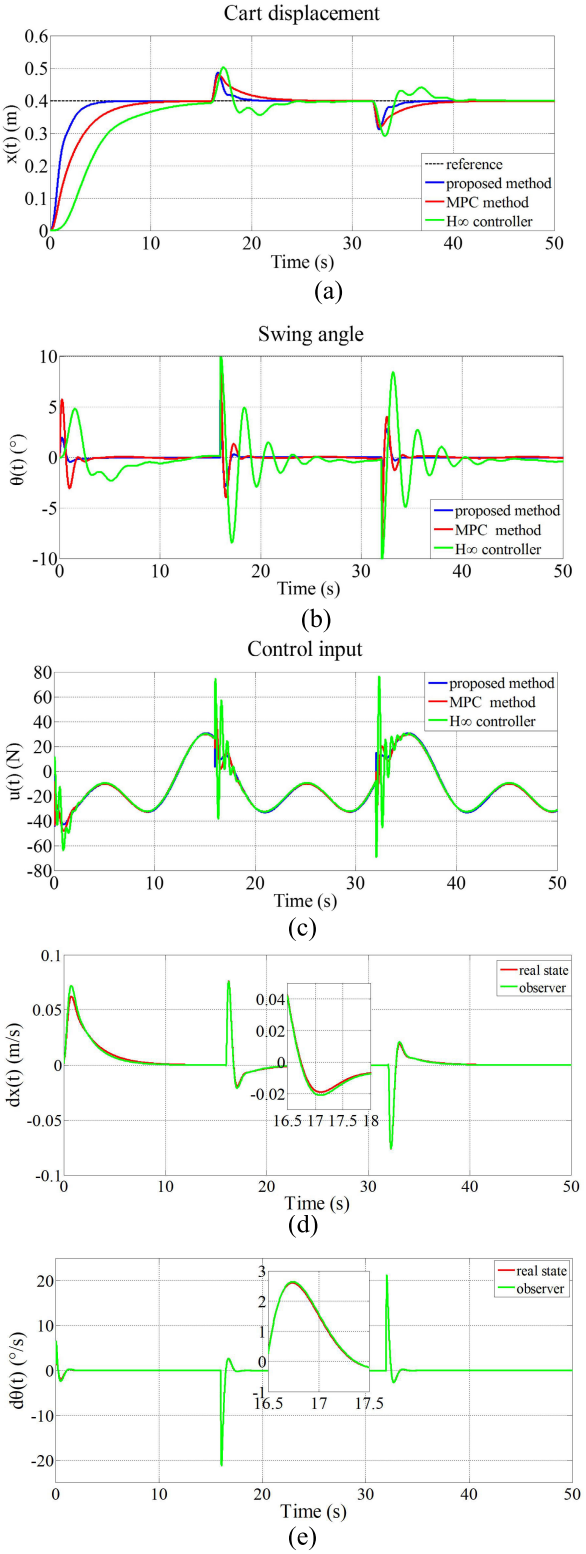

FIGURE 8. Comparison of the proposed method, existing MPC method, and standard H∞ controller for case 5; black dashed lines represent the reference, while the blue solid lines show the proposed method results. Red solid lines show the MPC method results, and the green solid lines results are representing the standard H∞ controller. (a) position. (b) swing angle. (c) control input using the three methods. (d) observed state of velocity. (e) observed state of swing angular velocity.

TABLE 1. MSE comparison of the three controllers in different cases.

Simulation conditons	Methods	MSE of swing angle
Case 1	the proposed method	0.00081
	the MPC method	0.00143
	Standard H_∞ controller	0.01034
Case 2	the proposed method	0.00174
	the MPC method	0.00875
	Standard H_∞ controller	0.02282
Case 3	the proposed method	0.00132
	the MPC method	0.00368
	Standard H_∞ controller	0.06329
Case 4	the proposed method	0.00315
	the MPC method	0.01068
	Standard H_∞ controller	0.14304
Case 5	the proposed method	0.00468
	the MPC method	0.01932
	Standard H_∞ controller	0.15281

performance and the lowest convergence time (compared to the existing MPC method and the standard H_∞ controller). Figure 5(d) and (e) illustrate the observed state of velocity and swing angular velocity.

In Case 3, two disturbance inputs, which are stochastic disturbances with the same amplitude, form, and duration, were manually imposed on the crane during the control process. The external disturbance was set to $d\,(t) = \pm 10$N, when $t = 16$s and $t = 32$s, meaning that twice transient disturbances with different directions were imposed on the crane during the control process.

The simulation results for each of the three methods in this group are shown in Figure 6. Figure 6(a) shows that the positioning error can be eliminated more quickly by using the proposed method compared to the existing MPC method. However, the highest oscillation and the longest convergence time were found there by using standard H_∞ controller. As shown in Figure 6(b), although there is no residual payload swing by using the existing MPC method and the proposed method, the latter had smaller angle oscillation. The largest angle oscillation was found in the standard H_∞ controller. Unlike the two described methods, the proposed method, not only removes the disturbances quickly but also eliminates the larger payload swings. Figure 6(d) and (e) illustrate the observed state of velocity and swing angular velocity.

In Case 4, two disturbance inputs were manually imposed on the playload during the control process. The external disturbance was set to $\theta\,(t) = \pm 10°$, when $t = 16$s and $t = 32$s, meaning that these disturbances were imposed on the payload during the control process.

The simulation results for each of the three methods in this group are shown in Figure 7. It was observed that the positioning error can be eliminated more quickly by using the proposed method compared to the existing MPC method in Figure 7(a). As shown in Figure 7(b), the proposed method had smallest angle oscillation and smallest convergence time. Figure 7(d) and (e) illustrate the observed state of velocity and swing angular velocity.

In Case 5, a comprehensive disturbance signal was used to evaluate the comprehensive performance for disturbance eliminating, in which the disturbance in Case 2 and Case 4 were imposed on the crane system simultaneously.

Based on the obtained results (Figure 8), although the disturbances were imposed on the crane and the playload at the same time, the proposed method has the best positioning performance and the anti-swing ability. Figure 8(d) and (e) illustrate the observed state of velocity and swing angular velocity. Table 1 gives a general overview of the comparison results from the three methods based on MSE. It can be seen that all the MSE of the proposed method are smaller than other two controllers in all five Cases.

Remark 1: Theoretically, it should be noted in Case 2 and Case 3 any type of unknown but bounded external disturbances can be attenuated by the proposed method. The design parameter values, such as disturbance attenuation coefficient γ, should be chosen properly to deal with larger disturbances.

Remark 2: It was shown in [33] that the double-pendulum crane systems with disturbances can be mathematically described as:

$$M(q)\ddot{q} + C(q,\dot{q})\dot{q} + G(q) = u + d \tag{42}$$

where $M(q)$ denotes the inertia matrix, $C(q,\dot{q})$ is the centripetal-coriolis matrix, $G(q)$ represents the gravity vector, and u is the control input vector. Due to $M(q)$ being invertible and positive definite, equation (40) could be rewritten as:

$$\begin{aligned}\ddot{q} = &-M_c(q)^{-1}C(q,\dot{q})\dot{q} + M_c(q)^{-1}u \\ &+M_c(q)^{-1}(d - G(q))\end{aligned} \tag{43}$$

Expression (41) can be rewritten as:

$$\dot{x} = \mathrm{A}x + Bu + D(t)$$

According to the above-presented analysis, it was predicted that the approach proposed in this paper can be applied to double-pendulum crane systems with disturbances. The authors aim to solve that problem in their future work.

V. CONCLUSION

In this paper, a novel H_∞ output-feedback control approach was developed and applied to deal with the non-linear overhead crane control problem with external disturbances. The non-linear system was expressed as a weighted sum of eight linear subsystems using the T-S fuzzy model. The virtual-desired variable synthesis was used to convert the tracking control into a stabilization problem, making the design procedure rather clear and easy. External disturbances were reduced by the H_∞ performance criterion. Furthermore, the simulation with three different case studies demonstrated the effectiveness of the proposed method in disturbance elimination. The results have shown in addition to quickly removing the disturbances, the proposed method has practically no positioning error with a smaller residual payload swing. The convergence time was 50% shorter compared to the MPC method, and one-third of the standard H_∞ controller convergence time. It should also be noted that, in theory, any type of bounded external disturbance can be reduced by using the proposed method. Thus, due to the good performance and simple structure, the proposed method can be easily used to actual control of the overhead crane systems. Meanwhile, the work in this paper provides a feasible idea for the crane control. Lastly, in the future work the authors aim to extend the proposed method to enable solving of the double-pendulum crane system with disturbances, which has a similar mathematical model with the overhead crane system.

APPENDIX A

The state vector was selected as $x = [x_1 x_2 x_3 x_4]^T = [x\theta\dot{x}\dot{\theta}]^T$, where u was the control variable. Next, model (1) was rewritten as:

$$(M+m)\dot{x}_3 + ml\left(\dot{x}_4\cos x_2 - x_4^2\sin x_2\right) = u - C_t x_3 + d \tag{A.1a}$$

$$m\dot{x}_3\cos x_2 + ml\dot{x}_4 + mg\sin x_2 = 0 \tag{A.1b}$$

Firstly, the authors calculated the value of (A.1a) $-$(A.1b)$\times$ $\cos x_2$ to obtain the following equation:

$$\left(M + m\sin^2 x_2\right)\dot{x}_3 = mg\cos x_2\sin x_2 - C_t x_3 + ml x_4^2\sin x_2 + u + d \tag{A.2a}$$

In the next step, we calculate (A.1b) $-$(A.1a) $\times$ $m\cos x_2/(M+m)$ to obtain:

$$\begin{aligned}l\left(M + m\sin^2 x_2\right)\dot{x}_4 = &-(M+m)g\sin x_2 + C_t\cos x_2 x_3 \\ &-ml x_4^2\sin x_2\cos x_2 - u\cos x_2 - d\cos x_2\end{aligned} \tag{A.2b}$$

By combining (A.2a) and (A.2b), state-space representation of the overhead crane was obtained (2).

REFERENCES

[1] X. Liang, Y. Fang, N. Sun, and H. Lin, "A novel energy-coupling-based hierarchical control approach for unmanned quadrotor transportation systems," *IEEE/ASME Trans. Mechatronics*, vol. 24, no. 1, pp. 248–259, Feb. 2019.

[2] C. Li, X. Pan, and G. Wang, "Torque tracking control of electric load simulator with active motion disturbance and nonlinearity based on T–S fuzzy model," *Asian J. Control*, vol. 22, no. 3, pp. 1280–1294, May 2020.

[3] W. Guo and D. Liu, "Nonlinear dynamic surface control for the underactuated translational oscillator with rotating actuator system," *IEEE Access*, vol. 7, pp. 11844–11853, 2019.

[4] H. Chen and N. Sun, "Nonlinear control of underactuated systems subject to both actuated and unactuated state constraints with experimental verification," *IEEE Trans. Ind. Electron.*, vol. 67, no. 9, pp. 7702–7714, Oct. 2020.
[5] M. Zhang, Y. Zhang, H. Ouyang, C. Ma, and X. Cheng, "Adaptive integral sliding mode control with payload sway reduction for 4-DOF tower crane systems," *Nonlinear Dyn.*, vol. 99, no. 4, pp. 2727–2741, Mar. 2020.
[6] M. J. Maghsoudi, Z. Mohamed, S. Sudin, S. Buyamin, H. I. Jaafar, and S. M. Ahmadc, "An improved input shaping design for an efficient sway control of a nonlinear 3D overhead crane with friction," *Mech. Syst. Signal Process.*, vol. 92, pp. 364–378, Aug. 2017.
[7] F. Li, C. Zhang, and B. Sun, "A minimum-time motion online planning method for underactuated overhead crane systems," *IEEE Access*, vol. 7, pp. 54586–54594, May 2019.
[8] L. A. Tuan, S.-G. Lee, V.-H. Dang, S. Moon, and B. Kim, "Partial feedback linearization control of a three-dimensional overhead crane," *Int. J. Control, Automat. Syst.*, vol. 11, no. 4, pp. 718–727, 2013.
[9] Z. Wu and X. H. Xia, "Optimal motion planning for overhead cranes," *IET Control Theory Appl.*, vol. 8, no. 17, pp. 1833–1842, 2014.
[10] H. Chen, Y. Fang, and N. Sun, "A swing constraint guaranteed MPC algorithm for underactuated overhead cranes," *IEEE/ASME Trans. Mechatronics*, vol. 21, no. 5, pp. 2543–2555, Oct. 2016.
[11] N. Sun, Y. Fang, and H. Chen, "A continuous robust antiswing tracking control scheme for underactuated crane systems with experimental verification," *J. Dyn. Syst., Meas., Control*, vol. 138, no. 4, Apr. 2016, Art. no. 041002.
[12] X. Wu and X. He, "Nonlinear energy-based regulation control of three-dimensional overhead cranes," *IEEE Trans. Autom. Sci. Eng.*, vol. 14, no. 2, pp. 1297–1308, Apr. 2017.
[13] H. Chen, B. Xuan, P. Yang, and H. Chen, "A new overhead crane emergency braking method with theoretical analysis and experimental verification," *Nonlinear Dyn.*, vol. 98, no. 3, pp. 2211–2225, Nov. 2019.
[14] M. Zhang, Y. Zhang, and X. Chen, "Finite-time trajectory tracking control for overhead crane systems subject to unknown disturbances," *IEEE Access*, vol. 7, pp. 55974–55982, 2019.
[15] I. P. Z. Setoodeh and M. H. Asemani, "Fault-tolerant tracking control of discrete-time T-S fuzzy systems with input constraint," *IEEE Trans. Fuzzy Syst.*, early access, Apr. 2, 2021, doi: 10.1109/TFUZZ.2021.3070573.
[16] X. Wu and X. He, "Partial feedback linearization control for 3-D underactuated overhead crane systems," *ISA Trans.*, vol. 65, pp. 361–370, Nov. 2016.
[17] Z. Wu, X. Xia, and B. Zhu, "Model predictive control for improving operational efficiency of overhead cranes," *Nonlinear Dyn.*, vol. 79, no. 4, pp. 2639–2657, 2015.
[18] A. Khatamianfar and M. Bagheri, "Application of independent joint control strategy for discrete-time servo control of overhead cranes," *J. Model. Simul. Elect. Electron. Eng.*, vol. 1, no. 2, pp. 81–88, 2015.
[19] T. Takagi and M. Sugeno, "Fuzzy identification of systems and its applications to modeling and control," *IEEE Trans. Syst., Man, Cybern.*, vol. SMC-15, no. 1, pp. 116–132, Feb. 1985.
[20] K. Tanaka, T. Ikeda, and H. O. Wang, "Robust stabilization of a class of uncertain nonlinear systems via fuzzy control: Quadratic stabilizability, H_∞ control theory, and linear matrix inequalities," *IEEE Trans. Fuzzy Syst.*, vol. 4, no. 1, pp. 1–13, Jan. 1996.
[21] P. Liu and T. S. Chiang, "H_∞ output tracking fuzzy control for nonlinear systems with time-varying delay," *Appl. Soft Comput.*, vol. 12, pp. 2965–2972, May 2012.
[22] C. C. Li, Y. F. Li, and G. L. Wang, "H_∞ output tracking control of uncertain and disturbed nonlinear systems based on neural network model," *Int. J. Syst. Sci.*, vol. 48, no. 10, pp. 2091–2103, Apr. 2017.
[23] H. Q. Xiao, Y. He, M. Wu, S. P. Xiao, and J. H. She, "New results on H_∞ tracking control based on the T–S fuzzy model for sampled-data networked control system," *IEEE Trans. Fuzzy Syst.*, vol. 23, no. 6, pp. 2439–2448, Mar. 2015.
[24] C. Zhang, J. Hu, J. Qiu, W. Yang, H. Sun, and Q. Chen, "A novel fuzzy observer-based steering control approach for path tracking in autonomous vehicles," *IEEE Trans. Fuzzy Syst.*, vol. 27, no. 2, pp. 278–290, Feb. 2019.
[25] H. D. Tuan, P. Apkarian, T. Narikiyo, and Y. Yamamoto, "Parameterized linear matrix inequality techniques in fuzzy control system design," *IEEE Trans. Fuzzy Syst.*, vol. 9, no. 2, pp. 324–332, Apr. 2001.
[26] B. Mansouri, N. Manamanni, K. Guelton, A. Kruszewski, and T. M. Guerra, "Output feedback LMI tracking control conditions with, H_∞ criterion for uncertain and disturbed T–S models," *Inform. Sci.*, vol. 179, no. 4, pp. 446–457, Feb. 2009.
[27] Z. W. Xu, H. Y. Su, H. L. Xu, and Z. G. Wu, "Asynchronous H_∞ filtering for discrete-time Markov jump neural networks," *Neurocomputing*, vol. 157, pp. 33–40, Jun. 2015.
[28] T. M. Guerra, A. Kruszewski, L. Vermeiren, and H. Tirmant, "Conditions of output stabilization for nonlinear models in the Takagi-Sugeno's form," *Fuzzy Set. Syst.*, vol. 157, no. 9, pp. 1248–1259, May 2006.
[29] Y.-C. Chang, C.-H. Chen, Z.-C. Zhu, and Y.-W. Huang, "Speed control of the surface-mounted permanent-magnet synchronous motor based on Takagi–Sugeno fuzzy models," *IEEE Trans. Power Electron.*, vol. 31, no. 9, pp. 6504–6510, Sep. 2016.
[30] C. Hildreth, "A quadratic programming procedure," *Naval Res. Logistics Quart.*, vol. 4, no. 1, pp. 79–85, 1957.
[31] Y.-S. Huang, W.-P. Liu, M. Wu, and Z.-W. Wang, "Robust decentralized hybrid adaptive output feedback fuzzy control for a class of large-scale MIMO nonlinear systems and its application to AHS," *ISA Trans.*, vol. 53, no. 5, pp. 1569–1581, Sep. 2014.
[32] R. Shahnazi, "Output feedback adaptive fuzzy control of uncertain MIMO nonlinear systems with unknown input nonlinearities," *ISA Trans.*, vol. 54, pp. 39–51, Jan. 2015.
[33] B. Lu, Y. Fang, and N. Sun, "Adaptive output-feedback control for dual overhead crane system with enhanced anti-swing performance," *IEEE Trans. Control Syst. Technol.*, vol. 28, no. 6, pp. 2235–2248, Nov. 2020.

CHENGCHENG LI received the B.S. degree in mechatronics engineering from Central South University, Changsha, China, and the M.S. and Ph.D. degrees in mechatronics engineering from Harbin Institute of Technology, Harbin, China.

He is currently a Lecturer in automatic control with Lanzhou Jiaotong University, Lanzhou, China. His current research interests include robust control and filtering, and analysis and control of nonlinear systems.

YUXIANG XIA received the B.S. and M.S. degrees in mechatronics engineering from Harbin University of Commerce, Harbin, China.

She has been a Lecturer in automatic control with Lanzhou Jiaotong University, Lanzhou, China. Her current research interests include process automation, control of nonlinear systems, intelligent control, and optimal control.

WENXUAN WANG received the Ph.D. degree in mechatronics engineering from Northwestern Polytechnical University, Xi'an, China.

He has been a Lecturer in automatic control with Lanzhou Jiaotong University, Lanzhou, China. His current research interests include robust control, process automation, and the control of nonlinear systems.